

Molecular Docking Based on Virtual Screening, Molecular Dynamics and Atoms in Molecules Studies to Identify the Potential Human Epidermal Receptor 2 Intracellular Domain Inhibitors

B. Ghalami-Choobar^{a,b,*} and H. Moghadam^b

^aDepartment of Chemistry, Faculty of Science, University of Guilan, P.O. Box: 19141, Rasht, Iran

^bDepartment of Chemistry, University Campus 2, University of Guilan, Rasht, Iran

(Received 4 June 2017, Accepted 7 October 2017)

Human epidermal growth factor receptor 2 (HER2) is a member of the epidermal growth factor receptor family having tyrosine kinase activity. Overexpression of HER2 usually causes malignant transformation of cells and is responsible for the breast cancer. In this work, the virtual screening, molecular docking, quantum mechanics and molecular dynamics methods were employed to study protein-ligand interactions to be applied for drug design. The virtual screening was performed by docking among 762 chemicals derived from ZINC library to find specific inhibitors for active sites in HER2 intracellular. Among the best-ranked compounds in comparison with the crystallographic inhibitor pyrrolo [3,2-d] pyrimidine, five compounds resulted and compound 1 was further tested by molecular dynamics simulation and also quantum theory of atoms in molecules. The obtained results indicated that the interactions of compound 1 with the active site of HER2 TK are stronger than those of pyrrolo [3,2-d] pyrimidine. Root mean square deviation, root mean square fluctuation, radius of gyration and binding free energy were calculated to check and evaluate the stability and mobility of the simulated system.

Keywords: HER2, Drug design, Molecular dynamics, Molecular docking, Tyrosine kinase

INTRODUCTION

The human epidermal growth factor receptor 2 (HER2) is a 185 kDa transmembrane protein (p185), located at long arm of human chromosome 17 (17q12) with three distinct regions [1]. The first one is a cytoplasmic tyrosine kinase (TK), which phosphorylates the other proteins inside the cell and involves the signal transduction. The second is a single α -helix transmembrane domain, TM domains, composed more hydrophobic residues anchor these proteins firmly to the membrane and also participate in the functions. The third region, ectodomain, is an N-terminal extracellular domain, providing a ligand-binding site. In humans, HER family consists of four structurally related members, HER1 (ErbB1, also known as EGFR), HER2, HER3 (ErbB3) and HER4 (ErbB4) [2]. Among them, HER2 is the only member

that has no identified ligand, however, it is the preferred partner to form heterodimer with other HER members [3]. HER2, in comparison with other members, has the highest affinity to form a heterodimers in a wide range of signal transduction [2,3]. Dimerization derives a rapid and abrupt activation of receptor's cytoplasmic kinase domain via auto phosphorylation of tyrosine residues [4]. HER2 is expressed in many tissues [5] which play critical roles in regulating the cell growth, survival, differentiation, migration, angiogenesis and invasion in a complex manner. Mitogen-activated protein kinase (MAPK) pathway, phosphatidylinositol 3-kinase (PI3K) pathway and phospholipase C- γ (PLC γ) are three major pathways mediated by HER2 [6]. HER2 dimerization promotes the mislocalization and rapid degradation of p27Kip1, a cell-cycle inhibitor protein, resulting to cell-cycle progression [7-9]. Some membrane receptors like insulin-like growth factor receptor 1 can also activate HER due to complex

*Corresponding author. E-mail: B-Ghalami@guilan.ac.ir

forming with it [5,10]. After the development of trastuzumab (Herceptin™), an engineered anti-HER2 antibody, a variety of HER2 specific antibodies and small molecular inhibitors have been assessed in clinical trials [11]. Furthermore, the upstream and downstream of the HER2 signaling pathway are encouraging targets to block the signal and inhibit the tumor growth. The intracellular domain has about 500 residues made up of a cytoplasmic juxtamembrane (JM) linker, a TK domain and a carboxyl-terminal tail [12]. The carboxyl-terminal tail has six tyrosine residues, which are employed for trans phosphorylation [13,14]. HER2 also can directly or indirectly act as a transcription factor to increase the gene expression of Cyclin D1 [15], cyclooxygenase-2 (COX2) [16] and p53 [17]. Overexpression of HER2 usually leads to malignant transformation of cells and is responsible for about 25 to 30% of all breast cancer cases. This over-expression is also related to aggressive index of tumor, lymph node involvement, and elevation of resistance to endocrine therapy [18]. It demonstrated that inhibition of HER2 expression induced meaningful apoptosis in breast cancer cells [2]. In addition to the breast cancer, numerous studies have shown that HER2 over-expression is also involved in gastric [19-21], ovarian [22-24] and prostate cancers [25,26]. Nowadays, the wide range of techniques, including high throughput-screening, fragment based screening, X-ray crystallography, NMR, mass spectroscopy, bioinformatics, molecular modeling and molecular docking are occupied to develop the potent, novel inhibitors and drugs against a variety of diseases [27-31].

During the last decade, several methods such as virtual screening method have been used for rational drug design [32]. In 2012, Cortopassi *et al.* searched potential HER2 inhibitors used for treatment of other illnesses such as hepatitis bacterial infections and sexual impotence screened in Drug Bank. So, compounds similar to lapatinib and gefitinib selected by virtual screening analysis were subjected to 8.0 ns of molecular dynamics (MD) simulations [33]. However, an emphasis on the recent applications and the developing therapeutic benefits regarding erbB2 inhibition in the last 5-10 years of clinical studies has been reported [34].

Because of the time consuming and money costs in drug design and discoveries (approximately 800 million dollars per drug), it seems that the computational biology and

molecular modeling methods are the efficient strategies in the fields mentioned above [29]. Since the discovery of its important roles in tumorigenesis, HER2 has attracted enormous attention as a target for cancer treatment. However, the development of drug resistance within a year of treatment, and the appearance of truncated forms of HER2 (p95HER2 and HER2 Δ 16) have led a shift in focus of research to the targeting of the kinase domain for the development of therapeutics [2,35]. Therefore, it is possible to predict the interactions of chemical compounds (drugs) with proteins based on computational methods and select the compounds which their binding to the target is more probable. Then, binding of these compounds can be investigated in the laboratory or in live systems.

In this study, utilizing computational methods, we combined virtual screening, molecular docking, molecular dynamics (MD) simulation and quantum theory of atoms in molecules (QTAIM) studies to design the potent and influential inhibitors against cytoplasmic tyrosine kinase domain of HER2. The virtual screening was performed by docking among 762 chemicals. The three high ranked compounds were chosen and the best of which was finally further tested by molecular dynamics simulation and also quantum theory of atoms in molecules. The obtained results indicated that the interactions of compound 1 with the active site of HER2 TK are stronger than those of pyrrolo [3,2-d] pyrimidine. Root mean square deviation (RMSD), root mean square fluctuation, (RMSF) and radius of gyration (RG) were calculated to check and evaluate the stability and mobility of the simulated system using molecular dynamics simulation. In addition, modified molecular mechanics-Poisson Boltzmann surface area (MM-PBSA) algorithm was employed to calculate the interaction free energy between chemical inhibitor and compound 1 with HER2 /TK.

METHODS

Structures Preparation

The 3D structure of HER2 TK domain (PDB code: 3RCD) was retrieved from the Brookhaven protein data bank [34]. All water molecules and non-polar hydrogen atoms were removed, and atom charges were computed by Gasteiger-Marsili method [36]. Before docking study, to relax any closed contact, the structure was minimized by the

steepest descent method implemented in GROMACS 5.1 [37]. For virtual screening, the core structure of a dual inhibitor pyrrolo[3,2-d]pyrimidine scaffold [34], was selected as a template and the structures with 50% similarity to the template, named ZINC library, were retrieved from ZINC database about 762 structures [32]. Thereafter, the charges of molecules were calculated by Gasteiger-Marsili method. Finally, the 3D structures were provided for molecular docking studies.

Molecular Docking

Molecular docking of ZINC library to the active site of HER2 TK was carried out by Auto Dock Vina. This software is a virtual screening which works on the basis of empirical scoring functions. Auto Dock Vina can compute the grid maps in an automatic manner. In the development of Vina, a variety of stochastic global optimization approaches were explored, including genetic algorithms, particle swarm optimization, simulated annealing and others, combined with various local optimization procedures and special "tricks" to speed up the optimization [38]. The crystal structure of HER2 TK had a pyrrolo [3,2-d] pyrimidine analogue (Pyr) as a chemical inhibitor and its surrounding residues were defined as an Active site with geometric position ($X = 12.03$, $Y = 0.27$, $Z = 29.73\text{\AA}$) [34]. For each run, using a scoring function of Auto Dock Vina, the pose with the lowest binding energy was chosen for MD simulations and QTAIM.

MD Simulation

All MD simulations were carried out using GROMACS 5.1 package with AMBER 99SB force field [37]. The partial charges and topology files of inhibitors were produced by ACPYPE, a tool based on ANTECHAMBER [39,40]. Each system was solvated in a cubic periodic box (The components of the simulation boxes for the given systems were as follows: dimension $7 \times 7 \times 7$), with TIP3P water model [41], and then sufficient chlorine and sodium atoms were added to neutralize the system. Energy minimizations were accomplished with the steepest descent integrator and the conjugate gradient algorithm consecutively to attain a maximum force of less than $1000 \text{ kJ mol}^{-1} \text{ nm}^{-1}$ on any atom. A twin range cutoff scheme was assigned to evaluate short-range, non-bonded interactions, with van der Waals

and electrostatic interactions truncated at 1.4 nm and 0.9 nm, respectively. To treat the long-range electrostatic interactions, particle mesh Ewald (PME) method was utilized [42,43]. The temperature was set at 300 K using velocity rescaling with a stochastic term and coupling time constant of 0.1 ps [44]. This thermostat is comparable with Brenden coupling, with the same scaling using, but the stochastic term ensures that a proper canonical ensemble is produced [37]. The pressure was fixed at 1.0 atm using a Parrinello-Rahman barostat with a coupling constant of 2 ps [45]. MD simulations were conducted with a time step of 2 fs, and all bonds involving hydrogen atoms were constrained by a Linear Constraint Solver (LINCS). Number of iterations to correct the rotational lengthening in LINCS (lincs_iter) and highest order in the expansion of the constraint coupling matrix (lincs_order) was assigned 1 and 4, respectively. For MD simulations, an order of 4 usually is enough. Each system was equilibrated under a constant volume (NVT) ensemble (100 ps) and a constant pressure (NPT) ensemble (100 ps). All MD simulations were conducted for 30 ns. The trajectories were analyzed using VMD software [46] and the standard tools were implemented in the GROMACS package.

Binding Free Energy

The MM-PBSA is open source software, and was employed to calculate the free energy of binding between two defined groups. Recently, MM-PBSA algorithm has been utilized as a scoring function in computational drug design [47]. In this study, MM-PBSA algorithm was employed to calculate the interaction free energy between designed and crystal inhibitor and HER2 TK. The free energy of binding was calculated from the Eq. (1):

$$G_{\text{binding}} = G_{\text{complex}} - (G_{\text{protein}} + G_{\text{ligand}}) \quad (1)$$

In which, G_{complex} is the total free energy of the protein-inhibitor complex and G_{protein} and G_{ligand} are total free energies of the separated form of protein and inhibitor in solvent, respectively [31,47].

Quantum Theory of Atoms in Molecules

All calculations were performed by using GAMESS electronic structure package [48]. The structures of

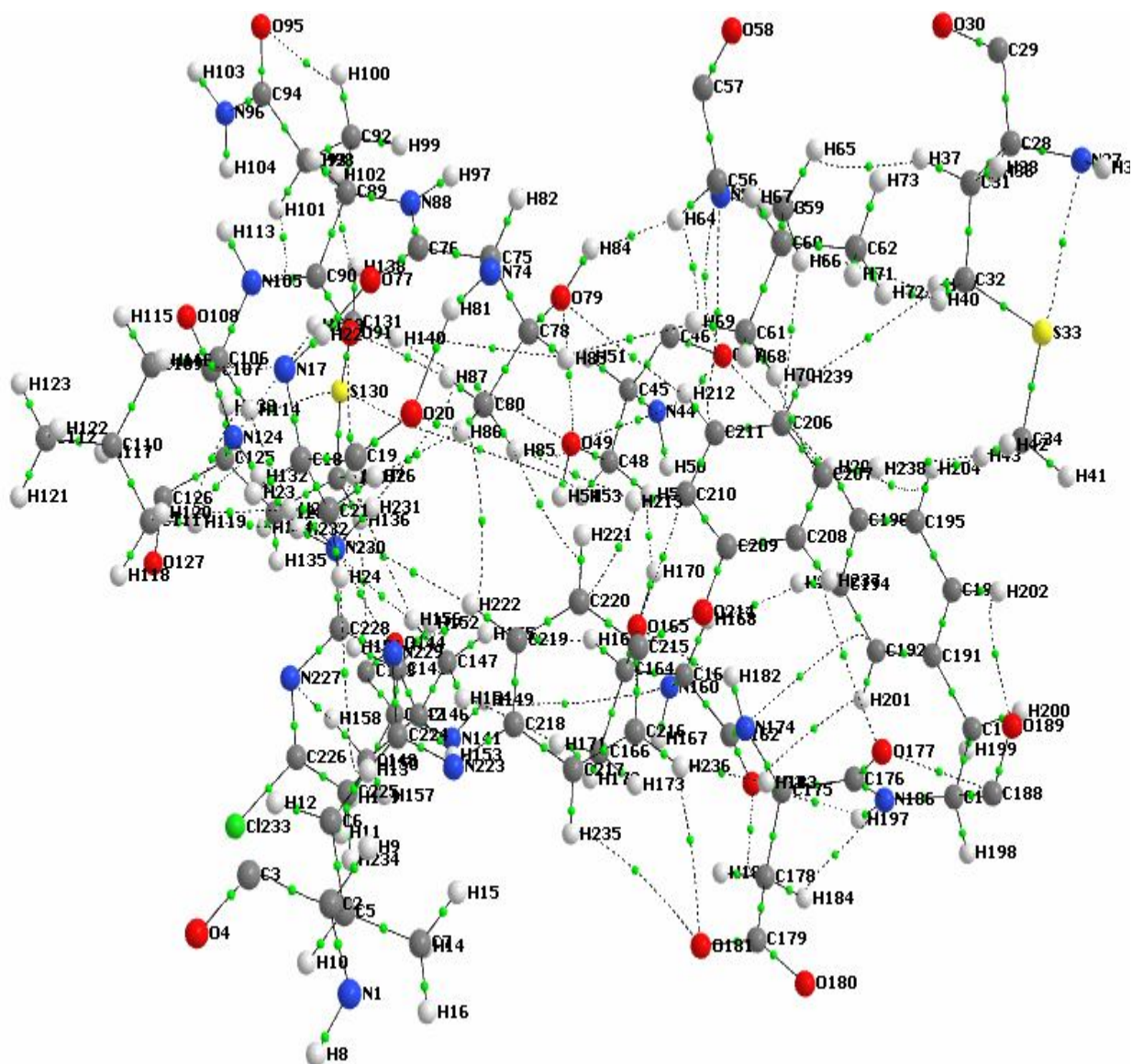
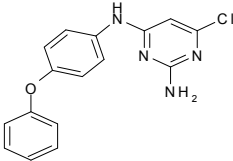
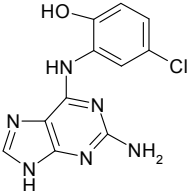
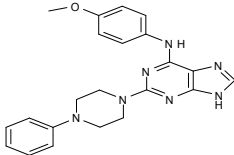
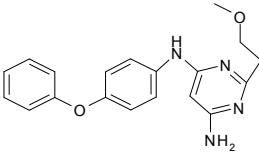
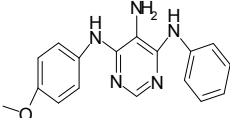
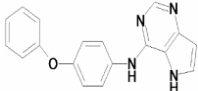


Fig. 1. Amino acid residues which form the active site of the HER2/COM1 at 4 Å distance away from COM1 (To more details see supporting information figure s26).

HER2/COM1 attained from docking section were optimized using ONIOM (B3LYP/6-31G**): Amber). Figure 1 shows amino acid residues which form the active site of HER2/COM1 at 4 Å distance away from substrate consisting of val734, Ala751, Met774, Leu785, Thr798, Gln799, Leu800, Met801, Leu852, Thr862, Asp863, Phe864 and Ser873 as well as the COM1 molecule. The mentioned residues were

cropped and then positions of all atoms were frozen. All atoms' energies were obtained using the M06-2X functional as recommended in literature [49]. The M06 family of hybrid exhibits the promise performance for exact studies of monovalent interactions in biological systems [50]. In this study, the basis set 6-31++G** was also used because theoretical studies have been shown that incorporation of

Table 1. Compound Structure, Zinc Database Code and Docking Energies of the Best Five Poses among 762 Structures, Achieved by Virtual Screening (mvd and autodock vina) and their Toxicity

Number	ZINK CODE	LIGAND	E (kcal mol ⁻¹)	MolDock Score	TOX ^a
(COM 1) A	ZINC01398025		-14.02	-121.619	495 mg kg ⁻¹
(COM 2) B	ZINC72240630		-11.31	-97.357	500 mg kg ⁻¹
(COM 3) C	ZINC32097318		-11.14	-95.119	125 mg kg ⁻¹
(COM 4) D	ZINC49467748		-10.25	-84.028	1000 mg kg ⁻¹
(COM 5) E	ZINC40781039		-9.93	-83.703	1600 mg kg ⁻¹
F	Pyrrolo[3,2-d]pyrimidine analogue [33]		-10.27	Template	

^aTo more details see supporting information tables s1-s11 and figures s1 s25.

different combinations of polarization and diffuse functions is crucial to describe precisely the hydrogen-bonded systems [51,52] and also the corresponding wave function was created at the M06-2X/6-31++G** level of theory. The QTAIM analysis was performed by AIMAll software [53].

RESULTS AND DISCUSSION

Docking Studies

The five top compounds obtained from virtual screening results are shown in Table 1. The calculated interaction energy between compound 1 (COM1) and HER2 TK active site is presented in Fig. 2A. As observed in Fig. 2A, the Phe 864 residue interacts with a phenoxy moiety of COM1 via π - π stacking. The Leu 800, Leu 726, Met 801 and Phe 1004 residues form a hydrophobic packet interacting with chloropyrimidine by hydrophobic interaction. Orientation and interaction energy of compound 2 is depicted in (Fig. 2B). The Leu 796 backbone is in H-bond contact with purine's NH₂ of compound 2. The Asp 863 interacts with OH and NH of compound 2 *via* two H-bonds. The phenyl moiety of compound 3 (Fig. 2C) and compound 4 (Fig. 2D) contributes in the π - π stacking with the Phe 864 residue. As seen in Figure 4, Ala 751, Leu 800, Met 801, Val 734, Phe 1004 and Leu 852 make hydrophobic interactions with compound 3. The Val 773, Met 774, Gly 776, Val 777, Gly 778, Val782, Ile 861, Thr 862, Phe 864 and Leu 866 residues form a hydrophobic packet in HER2 TK [12]. These hydrophobic interactions have been described by several groups in relation to its association with various molecules, together with, the molecular chaperone Hsp90 [54,55]. As depicted in Fig. 2D, Leu 796, Ala 751, Ile 752, Leu 800 formed a hydrophobic packet in vicinity of compound 4. The same hydrophobic interactions are also formed between HER2 TK and compound 5 (Fig. 2E). The Asp 863 is in H-bond contact with compound 5. The obtained docking results pointed out that Phe 864, Met 801, Ala 751, Val 734, Leu 800 and Asp 863 are important residues in maintaining the energetic conformations of the compounds studied inside HER2 TK because they are involved in Hydrogen-bond and hydrophobic interactions with most of the compounds. However, hydrophobic interactions play an important and critical role in the inhibitor-protein interaction [12]. Then, FAF-Drugs

program which is a free adaptable tool for ADMET (absorption, distribution, metabolism, excretion and toxicity) was used for filtering of electronic compound collections. The results for toxicity of compounds are presented in (Table 1). However, ligand C and D were accepted such as the drug-like and ligand A is intermediate in according to Lipinski rule of five [30].

Flexibility and Mobility Study

After docking studies, the COM1 (with -14.02 kcal mol⁻¹ docking energy) was selected by virtual screening analysis along with HER2 TK. The free HER2 TK and HER2 TK: Pyr complex were subjected to 100 ns in MD simulation. MD simulation provides a better picture of the overall stability of the HER2 TK and HER2 TK complex with COM1 and/or Pyr on a nanosecond time scale. The RMSD, RMSF and RG were employed to check and evaluate the stability and mobility of the simulated system. The RMSD is a crucial parameter to examine the equilibration of MD trajectories [56]. The values of RMSD in free HER2 TK, HER2 TK: Pyr and HER2 TK: COM 1 complexes are shown in Fig. 3. For the free HER2 TK, after a sharp rise of RMSD to 3.5 Å at 1164 ps, it decreased to 2 Å. Then, it gradually increased during the simulation process. In the case of the HER2 TK: Pyr complex, the RMSD values steadily increased to 3.1 Å at 45582 ps. After that, it decreased to 2.2 Å, followed by a slow increase up to 2.9 Å. Finally, the system achieved to the equilibrium state at 64400 ps. Upon Fig. 3, the RMSD of HER2 TK: compound 1 complex elevated to 2.3 Å at 27120 ps. Then, it was slowly decreased to 1.9 Å at 30480 PS, after that it raised to 2.7 Å at 43830 ps. Finally, the equilibrium state achieved at 45780 ps. According to Fig. 3, the decrease in the RMSD value of the complex from that of the free HER2 TK implies the stability of HER2 TK binding with Pyr or COM1.

Prior studies showed a particularly high degree of flexibility in α -helix C of HER2 TK compared to other HER family members [57]. So, the flexibility of HER2 TK backbone could be due to its α -helix C. Another possibility is that the crystal structure of HER2 TK relaxes in solution [30]. The RMSF with regard to the average MD simulation conformation is employed as a mean describing flexibility differences among residues [56]. The RMSF values of free

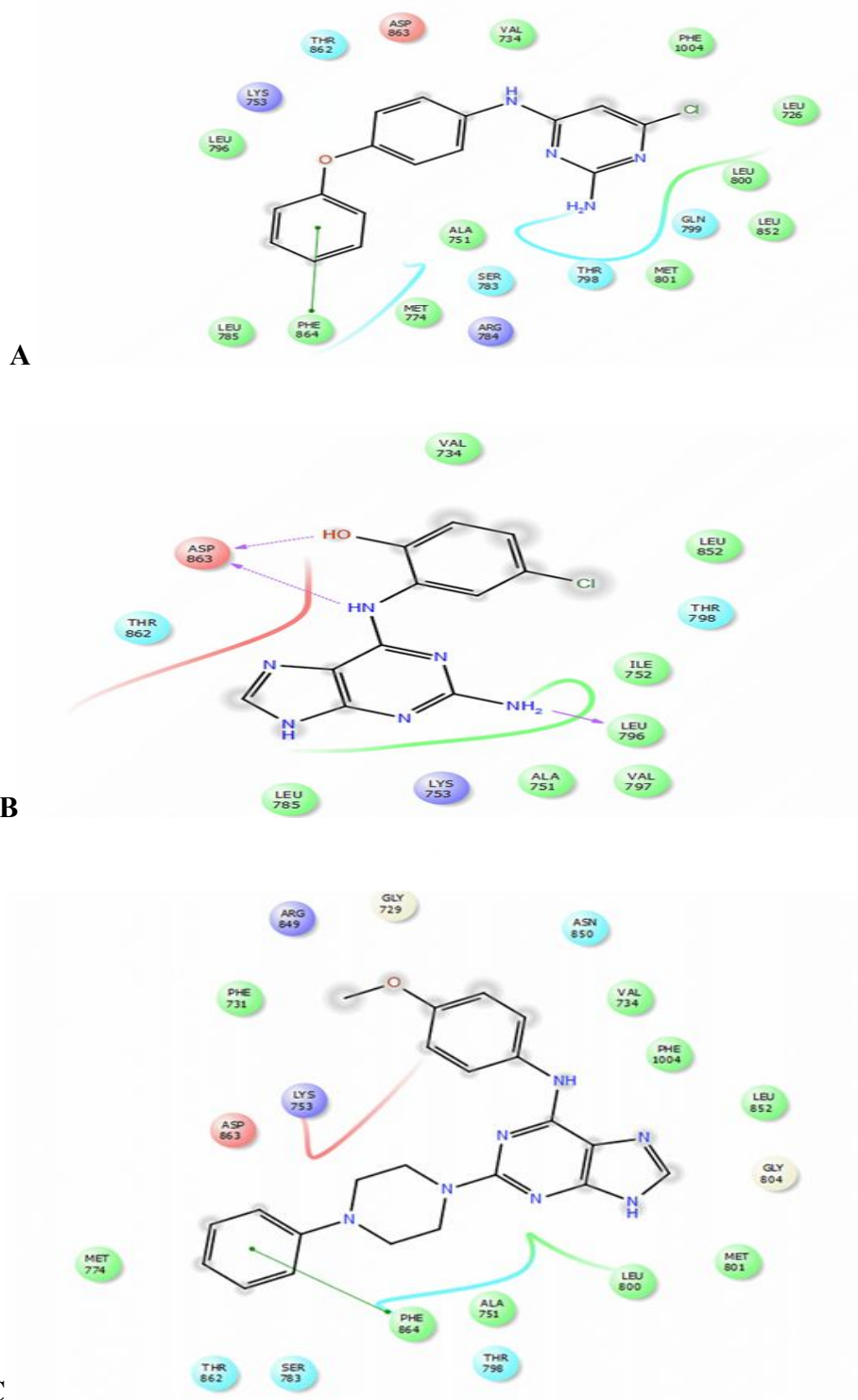


Fig. 2. Schematic two-dimensional representations of the binding interactions between compound 1 and HER2 TK active site (A), compound 2 and HER2 TK active site (B), compound 3 and HER2 TK active site (C), compound 4 and HER2 TK active site (D), compound 5 (E) (To more details see supporting information tables s12-s21 and figures s27).

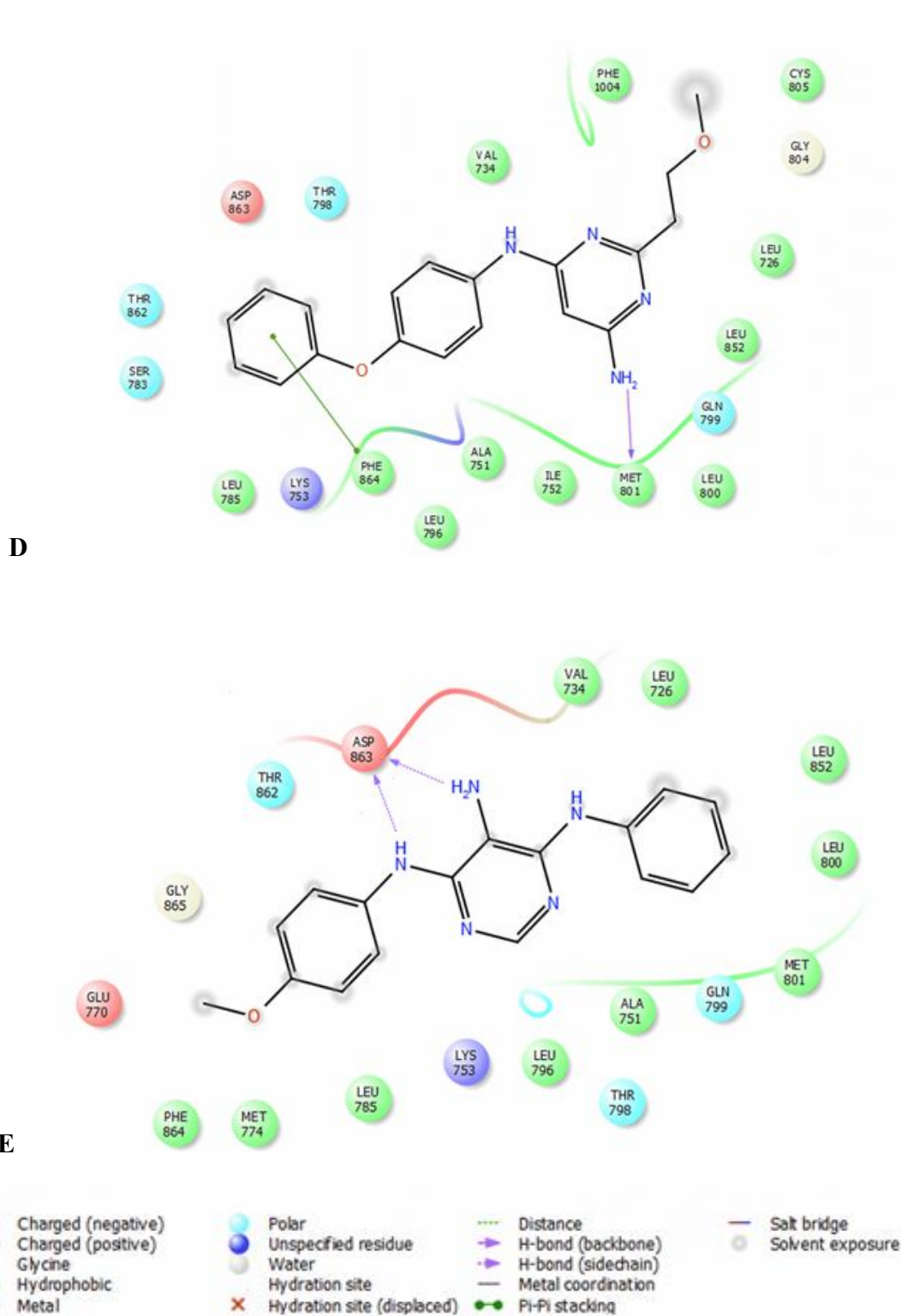


Fig. 2. Continued.

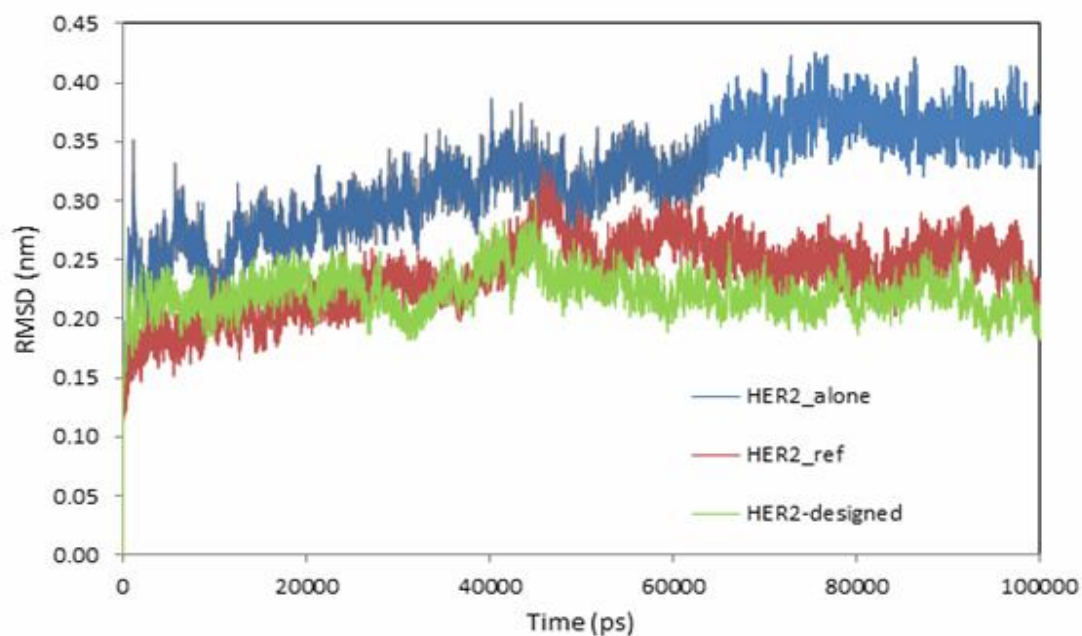


Fig. 3. Temporal RMSD values of free HER2 TK (a-blue line), HER2 TK: Pyr (b-red line) and HER2 TK: compound 1 (c-green line).

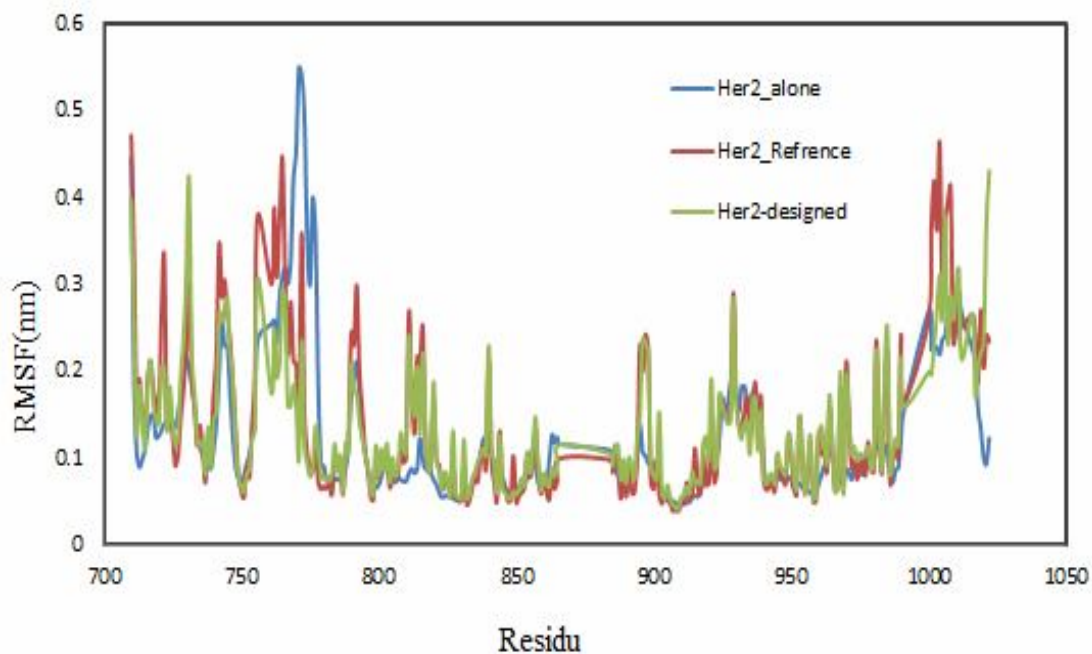


Fig. 4. RMSF of residues during MD simulation, RMSF comparison between free HER2 TK (a-blue line), HER2 TK: Pyr (b-red line) and HER2 TK: compound 1 (c-green line).

Table 2. Molecular Energy Terms for the HER2 TK: Pyr and HER2 TK: Compound 1 Complex

Energy (kcal mol ⁻¹)	HER2 TK : Pyr	HER2 TK : compound 1
ΔE_{vdw}	-200.027	-270.546
ΔE_{elect}	-44.119	-12.09
ΔE_{solv}	170.231	68.967
ΔE_{SASA}	-31.714	-19.908
$\Delta G_{\text{binding}}$	-105.629	-233.577

vdw, van der Waals; elect, electrostatic; solv, polar solvation; SASA, solvent-accessible surface area.

HER2 TK HER2 TK: Pyr/compound 1 complexes are depicted in Fig. 4. As seen in Fig. 4, the N-terminus of all systems has the high flexibility, which is predictable due to being free in one side (Figs. 4a, 4b and 4c). To influence phosphoryl transfer of the γ -phosphate of ATP to tyrosine residues on target substrates, several critical loops inside the kinase domain must be properly oriented [58]. Residues 727-732 (nucleotide-binding loop, or N-loop), which is a glycine-rich region [57], and 761-775 (α C helix) are responsible for coordination of the ATP and substrate tyrosine [12]. Following the binding of Pyr to HER2 TK, the RMSF values, in comparison with free HER2 TK, approximately remained unchanged (Figs. 4a and 4b). However, binding of compound 1 to HER2 TK increased the RMSF in N-loop (Fig. 4c). In the presence of Pyr or compound 1 in the active site of HER2 TK, the RMSF value of α C helix strongly decreased (Figs. 4b and 4c). For instance, the RMSF value of 5.4 Å in residue 771 (free HER2 TK), reduced to 1.5 and 0.9 Å by Pyr and compound 1, respectively (Fig. 4). Catalytic loop (C-loop), which is critical in promoting the phosphoryl transfer, consists of residues 844-850 [12]. Based on our data, RMSF value of Arg 844, which is located in C-loop, increased from 0.7 Å (free HER2 TK) to 1.3 and 1.2 Å in HER2 TK: Pyr complex and HER2 TK : compound 1 complex, respectively (Fig. 4). Fig. 5 demonstrates the Rg of HER2 TK in free or complex with Pyr and compound 1. Rg calculation was done to compute the HER2 TK compactness in different systems. The Rg is described as the mass weighted root

mean square distance of a collection of atoms from their common center of mass [56]. According to (Fig. 5), the Rg value of free HER2 TK varies between 19.1 and 20.6 Å. With regard to presented data, temporal Rg variation of HER2 TK, in the presence of Pyr or compound 1 is lower than free HER2 TK. All HER2 TK structures have the typical kinase bi-lobed folding. The N-terminal lobe (N-lobe) includes mostly β -strands and one α -helix, whereas the C-terminal lobe (C-lobe) is predominantly comprises of α -helical. The two mentioned lobes are joined by a flexible hinge region and separated by a deep cleft including the ATP binding site [57]. It can be concluded that free HER2 TK has much variation in Rg due to its hinge conformational changes. Such spatial changes may increase the chance of ligand binding to the HER2 TK binding site.

Details of the interaction between HER2 TK and compound 1 after 100 ns MD simulation are illustrated in (Fig. 6). Before MD simulation, Phe 864 interacts with compound 1 *via* π - π interaction (Fig. 2A). However, after 100 ns MD simulation, this residue is replaced with Glu799, Thr 798 and Met 801. It shows that Met 801 and Thr 862 interact with crystal Pyr *via* hydrogen bonding [57]. It should be noted that HER2 TK Thr 798 is involved in clinical drug resistance [59].

Binding Free Energy

To calculate the interaction free energy between Pyr/compound 1 and HER2 TK, MM-PBSA method was used as reported in literature [31]. Binding free energy

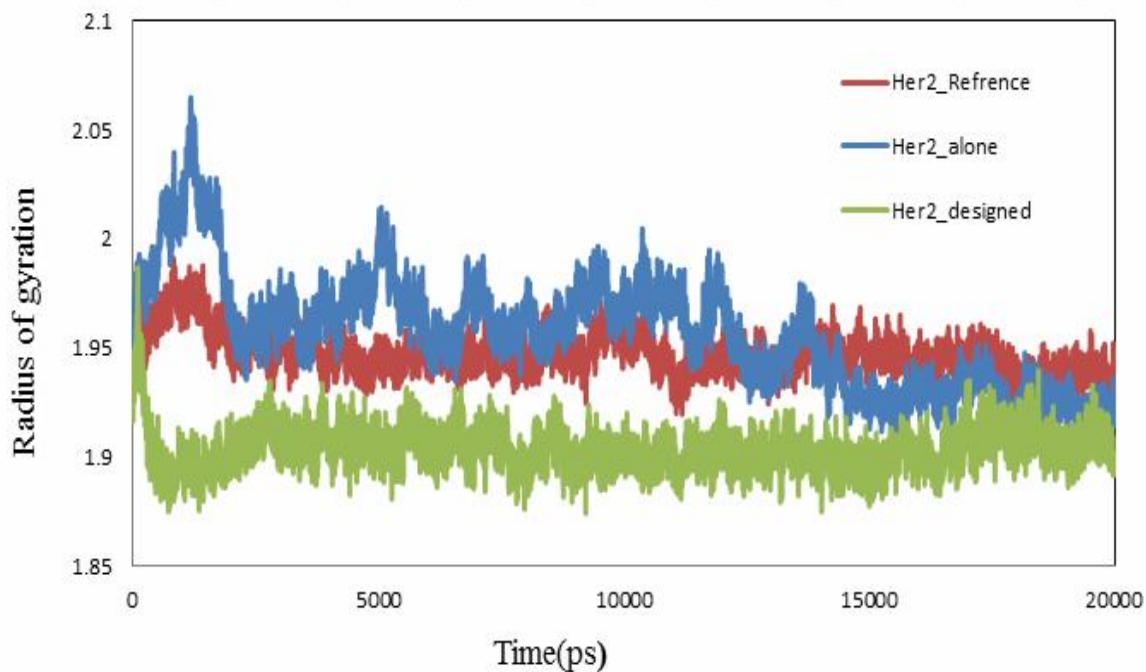


Fig. 5. Temporal radius of gyration values of free HER2 TK (a-blue line), HER2 TK: Pyr (b-red line) and HER2 TK: compound 1 (c-green line).

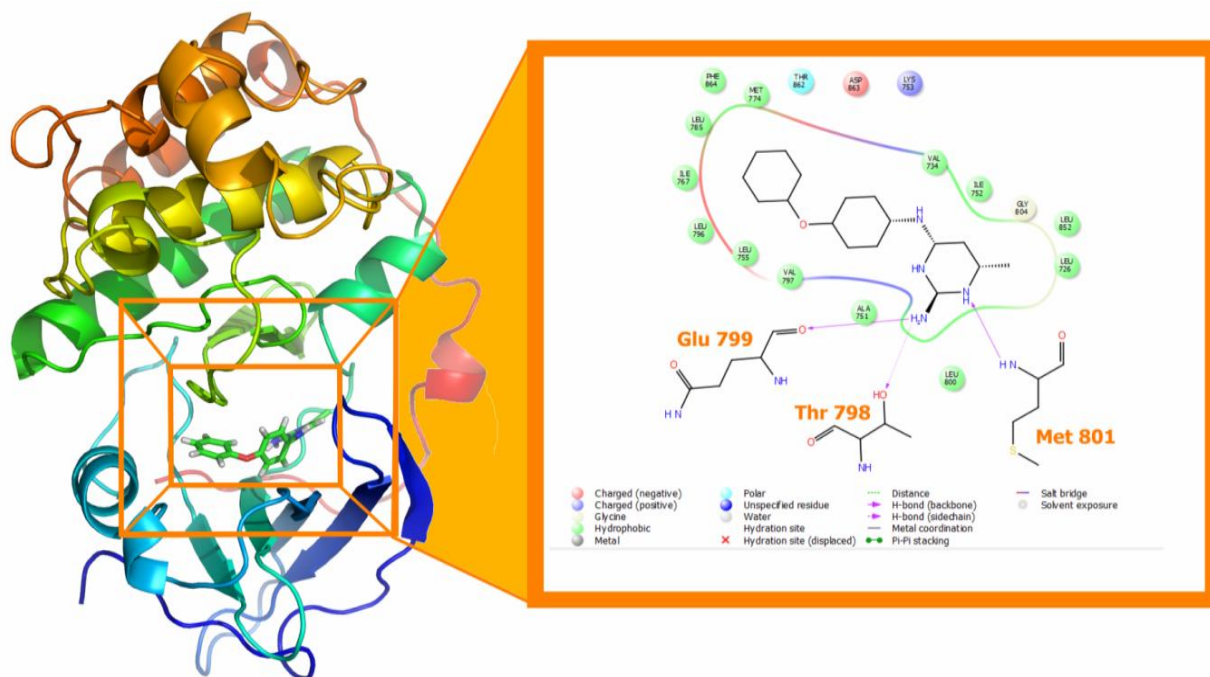


Fig. 6. The computed binding modes of compound 1 in the HER2 TK active site after 100 ns MD simulation.

computation demonstrated the affinities of each ligand to the HER2 TK binding site [33]. The snapshots were extracted from the last 20 ns of MD trajectories for the analysis of the binding free energy. In Table 2, the binding free energy of Pyr and compound 1 with HER2 TK are -105.629 and -233.577, respectively. The obtained results showed that polar and van der Waals energies are the most effective energies (under equal conditions), which favors in the binding of Pyr and COM1 to the binding site of HER2 TK. In addition, the total number of H-bonds in the HER2 TyK: COM1 complex versus time at 300 K is shown in Fig. 7A. The HER2 TyK: COM1 complex exhibited 2-3 H-bonds throughout the simulation time period. Moreover, the number of hydrogen bonds between the HER2 TyK: COM1 complex and water molecules were similar to free HER2 TyK and water molecules (see Figs. 7B and C). However, H-bond interactions were studied to more detail using AIM analysis (see section 3.4).

AIM Analysis

The Bader theory has been known as a valuable tool for analyzing hydrogen bonds. The analysis of the bond critical points (BCPs) properties is generally performed to estimate the hydrogen bond nature [60-65]. The parameters such as Laplacian of the electron density $\nabla^2\rho$, the electron energy density H that is the sum of the kinetic electron energy density (T) and the potential electron energy density (V), and also $-T/V$, derive from the Bader theory and imply the type of interaction. According to the properties of electron density distribution in the BCP [66,67],

$$E = 0.5 V \quad (2)$$

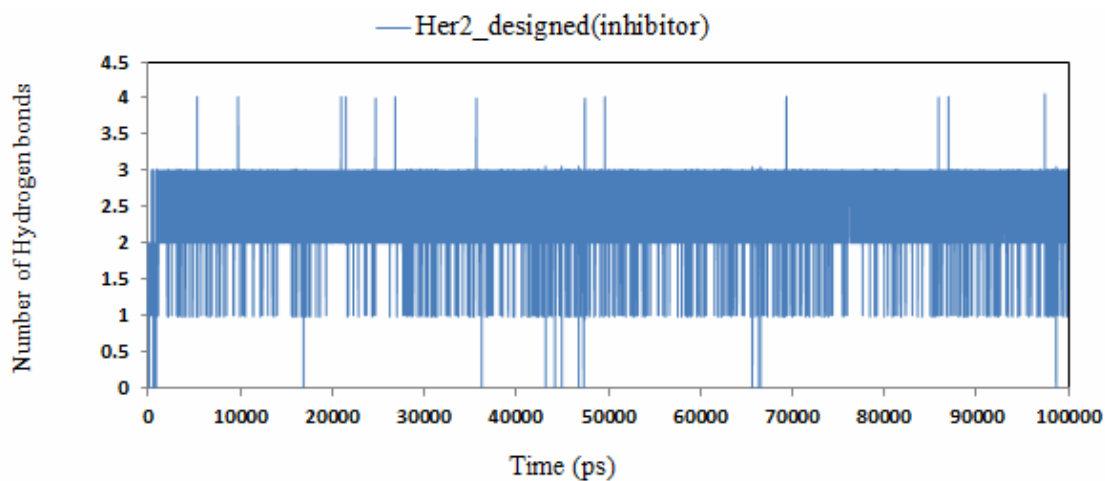
where V is the local potential energy value at the BCP for interaction. The negative value of a Laplacian undoubtedly infers a wholly covalent interaction. If both $\nabla^2\rho$ and H_{BCP} simultaneously be positive show that the interaction nature is non-covalent such as, van der Waals, ionic, Hydrogen bond (HB) interaction, dihydrogen bonding, etc. Therefore, if the value of ρ_{BCP} is in the range of 0.002-0.035 a.u., the presence of HB interaction is proved [68]. If $\nabla^2\rho$ be positive while H is negative, and $-T/V$ be smaller than 1, then the interaction character is considered as partly covalent [69-72].

Pyrimidine as a Lewis base can form hydrogen bond. In Table 3, electron concentration on the C225 causes to reaction with H11 from the methyl group of Val734 residue and, therefore, the C-H $\cdots \pi$ hydrogen bond is observed. The length and energy of this interaction are 3.18 Å and -1.71 kJ mol⁻¹, respectively, as reported in Table 3. In this case, the ρ value is 0.00307 and $-T/V$ is greater than unity. Furthermore, H has a small positive value, so interaction can be considered as a noncovalent.

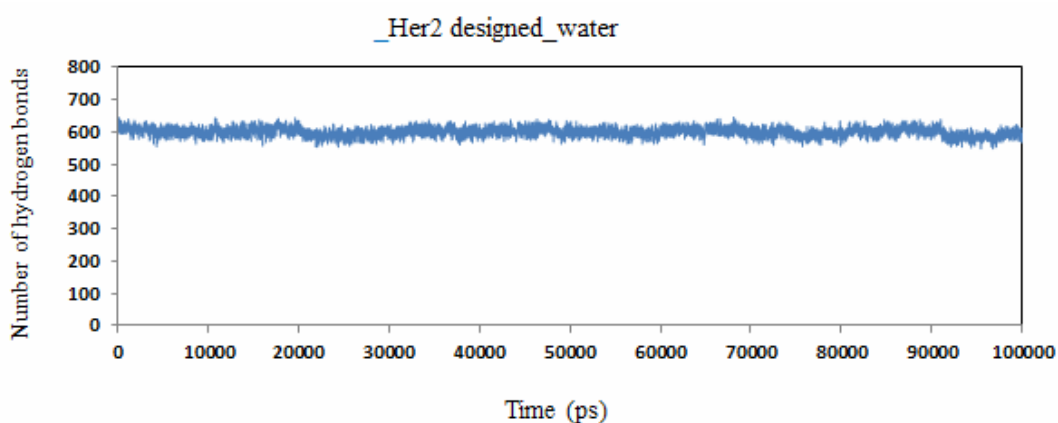
Considering Ala751 residue, C21 from the methyl group of amino acid has an interaction with N229 of pyrimidine ring. The nature of this interaction is van der Waals. Moreover, there is an interaction between the methyl group's H25 with N230 of amine group. Its distance and energy are 2.82 Å and -5.88 kJ mol⁻¹, respectively. As can be seen in Table 3, the positive values of $\nabla^2\rho$ and H indicate that the type of this interaction is noncovalent and due to the essence of interacting atoms this is a hydrogen bonding interaction. Because of the nitrogen atoms presence in pyrimidine, electron donor ability of NH₂ group is reinforced and Lewis base property improved, as a result, the strength of this interaction is much more than that of other hydrogen-nitrogen, hydrogen-oxygen and hydrogen-carbon interactions.

Besides the mentioned interactions, the methyl group's C21 of alanine residue also has an interaction with H222 of ring1 in (Fig. 8). The interaction energy (E) is -1.71 kJ mol⁻¹ and its length is 3.3 Å. From data shown in Table 3, the values of $\nabla^2\rho$ and H are positive indicating that this interaction is noncovalent in nature and since the ρ value is in the range of hydrogen bonding, it can be concluded that this is a hydrogen bond interaction.

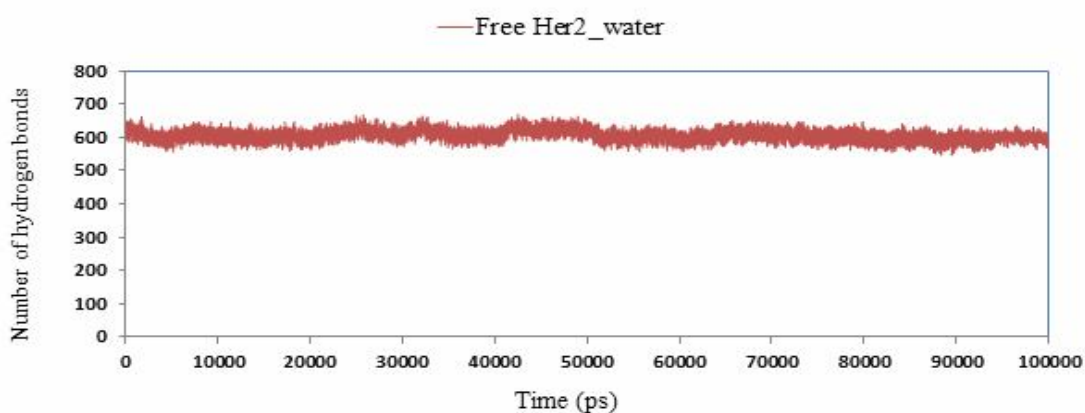
Met774 residue undergoes two interactions with the hydrogens of phenolic ring as H39-H239 and H43-H238 having 3.27 Å and 2.38 Å bond lengths, respectively. Because of this fact that the oxygen atom on the ring is an electron donor and para directing group, it is expected that the interaction of H39 and H239 be stronger than H43-H238. The obtained interaction energy values are -0.69 and -3.6 kJ mol⁻¹ for H39-H239 and H43-H238, respectively. According to the positive amounts of $\nabla^2\rho$ and H , it can be deduced that these interactions have noncovalent nature. The comparison of the ρ values reveals that the interaction



A



B



C

Fig. 7. Number of Hydrogen Her2 designed(A), Her2_designed-water(B) and Free HER2-water(C) from A to C, respectively.

Table 3. Topological Properties at the BCP of HER2 Interactions with Com1 (such as, Van der Waals, HB Interaction, Dihydrogen Bonding)

Residue	Atoms	BPL	ρ	$\nabla^2\rho$	T	V	H	E	-T/V
		(Å)					(kJ mol ⁻¹)	(kJ mol ⁻¹)	
Val734	H11 - C225	3.18	0.00307	0.010032	0.001907	-0.00131	0.000601	-1.71	1.46
Ala751	C21 - N229	3.78	0.005089	0.01701	0.003488	-0.00272	0.000765	-3.57	1.28
	H25 - N230	2.82	0.007612	0.025355	0.005409	-0.00448	0.00093	-5.88	1.21
	C21 - H222	3.30	0.003076	0.010783	0.001998	-0.0013	0.000697	-1.71	1.54
Met774	H39 - H239	3.27	0.001241	0.004251	0.000793	-0.00052	0.00027	-0.69	1.52
	H43 - H238	2.38	0.005685	0.021178	0.004017	-0.00274	0.001278	-3.60	1.47
Ser783	O47 - H212	2.69	0.00668	0.026024	0.00537	-0.00423	0.001136	-5.56	1.27
	O49 - H212	3.07	0.003002	0.013511	0.002512	-0.00165	0.000866	-2.16	1.53
Leu785	N55 - C211	3.96	0.002317	0.008216	0.001612	-0.00117	0.000442	-1.54	1.38
	H66 - C206	2.98	0.004714	0.014085	0.00275	-0.00198	0.000771	-2.60	1.39
	H70 - C207	2.80	0.007516	0.024103	0.004955	-0.00388	0.001071	-5.10	1.28
Thr798	H87 - H231	3.02	0.00172	0.007473	0.001284	-0.0007	0.000584	-0.92	1.83
	O79 - H212	3.36	0.001714	0.00821	0.001478	-0.0009	0.000575	-1.18	1.64
	H85 - C220	3.56	0.003707	0.012678	0.002406	-0.00164	0.000764	-2.16	1.47
	H86 - H222	3.08	0.002942	0.010443	0.001968	-0.00133	0.000643	-1.74	1.49
Gln799	O91 - H231	3.05	0.002985	0.014855	0.00277	-0.00183	0.000944	-2.40	1.52
Leu800	H119 - H232	2.48	0.005405	0.020632	0.003934	-0.00271	0.001224	-3.56	1.45
Met801	H132 - H232	1.45	0.029567	0.084142	0.02535	-0.02966	-0.00431	-38.94	0.85
	H137 - N230	3.11	0.003625	0.012428	0.002441	-0.00178	0.000666	-2.33	1.37
Leu852	H156 - N230	2.93	0.005573	0.018303	0.00384	-0.0031	0.000736	-4.07	1.24
	H158 - N227	2.76	0.007429	0.02406	0.005107	-0.0042	0.000908	-5.51	1.22
Thr862	O165 - C216	3.75	0.003088	0.012107	0.002367	-0.00171	0.000659	-2.24	1.39
	H171 - C217	3.50	0.002371	0.007624	0.001469	-0.00103	0.000437	-1.35	1.42
Asp863	O181 - H235	3.40	0.001318	0.006463	0.001118	-0.00062	0.000498	-0.82	1.80
	O181 - H236	3.15	0.002307	0.009799	0.001714	-0.00098	0.000736	-1.28	1.75
	O177 - H237	3.77	0.000968	0.005075	0.000891	-0.00051	0.000378	-0.67	1.74
	H183 - H236	2.28	0.005265	0.021223	0.003911	-0.00252	0.001395	-3.30	1.55
Phe864	H205 - C206	3.34	0.003844	0.012278	0.002381	-0.00169	0.000689	-2.22	1.41

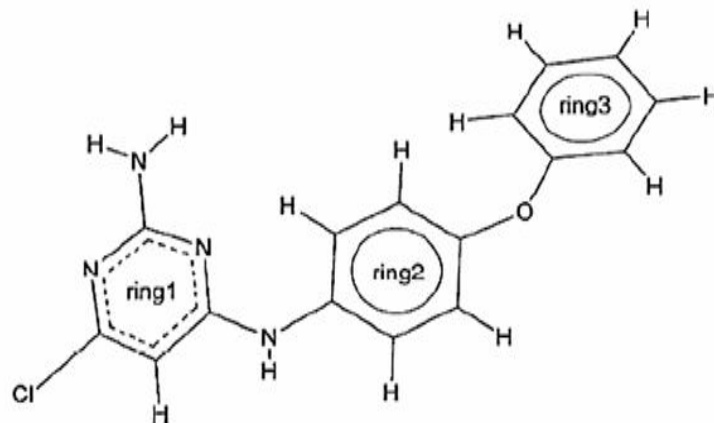


Fig. 8. Compound 1 (COM1) with Zinc code: ZINC01398025, which was selected as new potent inhibitors against HER2 TK in virtual screening.

of H39-H239 is a dipole-dipole whereas H43-H239 is a dihydrogen interaction.

Ser783 residue experiences two interactions with the COM1. In both cases H212 of COM1 interacts with O49 of hydroxyl group and O47 of carbonyl group. The interaction of carbonylic oxygen atom with H212 has the energy of $-5.56 \text{ kJ mol}^{-1}$ and its length is 2.69 \AA . According to BCP Parameters, this interaction is noncovalent and hydrogen bonding type. For the interaction of hydroxylic oxygen atom with H212 the interaction energy and length are $-2.16 \text{ kJ mol}^{-1}$ and 3.07 \AA . Similarly, the BCP parameters reveal that this interaction is noncovalent and hydrogen bonding type.

In Leu785 residue, N55 from amine group interacts with C211 of phenolic ring. The interaction energy and distance are $-1.54 \text{ kJ mol}^{-1}$ and 3.96 \AA , respectively. The BCP values display that this is a van der Waals interaction. The H66 of CH₂ group also has an interaction with C206 of phenolic ring. Its energy is $-2.60 \text{ kJ mol}^{-1}$ and interaction is 2.98 \AA in length. The values of $\nabla^2\rho$ and H are indicative of hydrogen bonding in nature and C-H... π interaction. As mentioned earlier, due to the existence of the electron donating OR substituent at *para* position of the ring making active the aromatic ring, the Lewis base property of C206 is enhanced and therefore a C-H... π interaction is formed.

Moreover, H70 of methyl group interacts with C207 of phenolic ring, its energy is $-5.10 \text{ kJ mol}^{-1}$ and the interaction

distance is 2.8 \AA . The topological values are manifestation of a hydrogen bonding interaction. This interaction is under the influence of dihydrogen interaction occurred between COM1 and Met744. So, it causes that a stronger C-H... π interaction is formed at *Meta* position of the ring.

In investigation on the nature of these interactions, the mentioned residues along with the COM1 molecule cannot be separated from the other *parts* of the HER2/COM1 and should be investigated as an integrated system. It seems that with individual study of residues and ligand, the effect of such interactions cannot be recognized.

THR is a hydroxylic residue, so it is expected that its hydroxyl group has a significant role in interaction with COM1. However, it is oriented in such a way that the carbonyl group is out of the interaction region. Therefore, interactions of COM1 with Thr798 residue are limited to the interaction of its methyl and OH groups.

First, there is a weak interaction between H87 of methyl group from Thr798 and amine group's H231 of Pyrimidine ring, the interaction energy is $-0.92 \text{ kJ mol}^{-1}$ and obtained BCP values indicate that this interaction is weaker than hydrogen bond which can be due to dipole -dipole interaction. Since the interaction between carbonyl group of Gln799 residue and H231 is stronger than this one, it can be concluded that in this interaction NH₂ group can act as a Lewis base and interaction between two Hydrogen atoms is formed.

Second, O79 of the -OH group from amino acid interacts with H212 of phenolic ring. Its interaction length and energy, respectively, are 3.36 Å and -1.18 kJ mol⁻¹. It is anticipated that this interaction is a hydrogen bonding interaction but the ρ value is smaller than 0.002 a.u. indicating that interaction is not hydrogen bonding type and is weaker than a conventional hydrogen bond.

Third, the interaction of H85 of methyl group with C220 of ring 2 has energy and distance of, respectively, -2.16 kJ mol⁻¹ and 3.56 Å. The effect of etheric oxygen atom (O214) on the ring 2 is as *ortho/para* directing and causes to activation of ring and C220 atom. As a result, a C-H... π interaction is formed. The calculated values of ρ , $\nabla^2\rho$ and H indicate that it is a hydrogen bonding interaction.

Another interaction seen in Thr798 is the interaction through methyl group's H86 atom of residue to H222 from ring 2. The bridged nitrogen atom between phenolic and pyrimidine ring serves as ring activator and *ortho/para* directing group and, therefore, leads to formation of a dihydrogen interaction with energy of -1.74 kJ mol⁻¹ and length of 3.08 Å. Considering the BCP values, given in Table 3, it can be found that this dihydrogen interaction is similar to hydrogen bond.

In the interaction of Gln799 with COM1, carboxyl group of amino acid interacts with amine group's H231. Here, interaction energy and distance are -2.40 kJ mol⁻¹ and 3.05 Å, respectively. From the information of Table 3, it is a hydrogen bonding interaction.

Leucine is known as an aliphatic residue. The methyl group of Leu800 has a dihydrogen interaction with hydrogen of amine group, a Lewis acid. With a brief look at the BCP values, it can be understood that this is in the range of hydrogen bond interaction.

The strongest interaction among presented interactions is the one between amine group of Met801 and H232 from amine group bounded to pyrimidine ring. The interaction occurred between two hydrogens of primary and secondary amine groups is N230-H232...H132- N124.

The calculated values of interaction energy and length are -38.9 kJ mol⁻¹ and 1.45 Å, respectively. Herein, $\nabla^2\rho < 0$ and $-T/V$ is smaller than 1 representing that although this interaction is dihydrogen, it is partial covalent in nature.

Another interaction of Met801 with COM1 belongs to H137 of residue's CH₂ and amine group's N230 of COM1.

Nitrogen as a primary amine plays the role of a strong Lewis base and directly leads to this interaction. The energy of this interaction is -2.33 kJ mol⁻¹ and its length is 3.11 Å. From the evidence of Table 3, this interaction can be regarded as a hydrogen bonding interaction.

Two methyl groups of Leu852 have interactions with amine group and pyrimidine ring. These interactions, respectively, belong to H156-N230 and H158-N227. Their interaction energies and lengths are -4.07, -5.51 kJ mol⁻¹ and 2.93, 2.76 Å, respectively. The nitrogen of NH₂ group in the H156-N230 interaction, as mentioned earlier, formed a stronger interaction than that of MET801.

The N227 of pyrimidine ring due to the electron donating of NH₂ group to the ring and also *ortho* position of N227 has Lewis base role and forms interaction with H158 of methyl group of residue 852. According to BCP values these are hydrogen bond interactions.

Two interactions can be recognized between Thr862 and COM1. First, the methyl group's H171 has interaction with C217 of ring 2. The C217 located in the *ortho* position of the bridged nitrogen can withdraw excess electrons of this atom and play the Lewis base role, so produces C-H... π interaction with energy of -1.35 kJ mol⁻¹ and length of 3.5 Å. The BCP parameters for this interaction show that this is a hydrogen bonding interaction.

Threonine is a hydroxyl amino acid, and existence of such structure activators lead to the formation of various interactions or interaction with a specific ligand. Herein, hydroxyl group in the residue structure leads to following noncovalent interaction: the interaction of O165 of OH group with ring 2 having energy and length of -2.24 kJ mol⁻¹ and 3.75 Å, respectively.

Aspartic acid is a charged amino acid and there is a high probability for the interaction between a charged group and COM1. Asp863 residue provides four interactions with COM1 including O181-H235, O181-H236, O177-H237 and O183-H236. In the first and second interactions carboxyl group's O181 of Asp863 interacts with H235 and H236 of phenyl ring (ring3). BCP parameters for O181-H235 are $\rho = 0.001318$, $\nabla^2\rho = 0.006463$ and $H = 0.000498$, demonstrating that nature of this interaction is noncovalent and also it is not hydrogen bonding in type. According to BCP parameters, O181-O236 interaction is a hydrogen bonding type. The carboxyl functional group having

negative charge in Asp residue exerts much influence on the hydrogen atom located near it than those located further. The electron donating and Ortho/Para donating property of -OR group on the ring cause that the interaction of O181 with H236 is stronger than one with H235.

For interaction of O177 of carbonyl group with H237 of ring 3, BCP parameters indicate that this interaction is so weak and also does not belong to hydrogen bonding type. The interaction of H183 and H236 of ring 3 has energy of $-3.30 \text{ kJ mol}^{-1}$ and length of 2.28 \AA . From the BCP parameters given in Table 3, this interaction is a noncovalent and dihydrogen in type.

In another residue, Phe864, the only interaction is the interaction of *para*-hydrogen of phenolic ring from amino acid with C206 of ring 3. Phenylalanine is an aromatic amino acid and electron transfer in structure can cause intermolecular interactions. The R group of phenol ring on residue 864 is a weak electron donating group, so it is expected that the interaction between phenol and phenyl rings is not very strong, while the aromaticity of residue activated phenol ring (ring 3) and also density of electrons on C206 atom lead to C-H... π interaction having interaction energy and length of $-2.22 \text{ kJ mol}^{-1}$ and 3.34 \AA , respectively. The obtained values of $\nabla^2\rho$ and H are positive for this interaction meaning that this interaction is noncovalent. On the other hand, the ρ value is 0.003844 showing that this interaction is in the range of hydrogen bonding interaction.

CONCLUSIONS

HER2 is employed as a prognostic and biomarker in breast and gastric/gastroesophageal cancers. Through computational methods, it is possible to predict the interactions of chemical compounds (drugs) with proteins and select the compounds which their binding to the target is more probable. Then, binding of these compounds can be investigated in the laboratory or in live systems. We performed our simulations on a set of 762 molecules selected in the Zinc basing based on the structural similarity with the crystal HER2 TK inhibitor: Pyr. The docking was performed and the parent compound was also used as control in the docking experiments. The ranking of best poses by docking score show three molecules with a lower

energy of crystal inhibitor. COM1 was further investigated and compared with the interaction mode of the lead compound Pyr using MD simulation. Based on the stability of the complex HER2 TK, it can be concluded that in similar conditions COM1 is much similar than parent compound. In the present study, we proposed the competitive inhibition mechanism with HER2 TK: Pyr. We also found new potent inhibitors against HER2 TK with virtual screening. The Binding free energy computation confirmed that the COM1 is more potent than parent crystal inhibitor. It can be also concluded that the structures investigated are promising candidates to develop and introduce new chemotherapies for the treatment of cancer based on HER2 inhibitors. The number and type of interactions were characterized by using quantum mechanics calculations method and quantum theory of atoms in molecules (QTAIM). The obtained results present that this treatment for interaction screening by docking and molecular mechanics software cannot clearly identify the number, type and energy of interactions whereas quantum mechanics method helps us to attain this goal. Total bonding energy of COM1 ligand was obtained equal to $-108.81 \text{ kJ mol}^{-1}$. This value represents the amount of interaction or bonding energy of ligand with protein.

ACKNOWLEDGEMENTS

We gratefully acknowledge the graduate Office University of Guilan for supporting of this work.

REFERENCES

- [1] Brandt-Rauf, P. W.; Pincus, M. R.; Carney, W. P., The c-erbB-2 protein in oncogenesis: molecular structure to molecular epidemiology, *J. Crit. Rev. Onc.* **1994**, *5*, DOI: 10.1615/CritRevOncog.v5.i2-3.100
- [2] Tai, W.; Mahato, R.; Cheng, K., The role of HER2 in cancer therapy and targeted drug delivery, *J. Control Release.* **2010**, *146*, 264-275, DOI: 10.1016/j.jconrel.2010.04.009.
- [3] Rubin, I.; Yarden, Y., The basic biology of HER2, *J. Ann. Oncol.* 2001, *12*, S3-S8, DOI: https://doi.org/10.1093/annonc/12.suppl_1.S3.

- [4] Satyanarayanajois, S.; Villalba, S.; Jianchao, L.; Lin, G. M., Design, synthesis, and docking studies of peptidomimetics based on HER2-Herceptin binding site with potential antiproliferative activity against breast cancer cell lines, *J. Chem. Bio. Drug.* **2009**, *74*, 246-257, DOI: 10.1111/j.1747-0285.2009.00855.x.
- [5] Iqbal, N.; Iqbal, N., Human epidermal growth factor receptor 2 (HER2) in cancers: overexpression and therapeutic implications, *J. Mol. Cell Biol.* **2014**, 2014.
- [6] Neve, R.; Lane, H.; Hynes, N., The role of overexpressed HER2 in transformation, *J. Ann. Oncol.* **2001**, *12*, S9-S13, DOI: https://doi.org/10.1093/annonc/12.suppl_1.S9.
- [7] Citri, A.; Yarden, Y., EGF-ERBB signalling: towards the systems level, *J. Nat. Rev. Mol. Cell. Biol.* **2006**, *7*, 505-516, DOI: 10.1038/nrm1962.
- [8] Moasser, M. M., The oncogene HER2: its signaling and transforming functions and its role in human cancer pathogenesis, *J. Oncol.* **2007**, *26*, 6469-6487.
- [9] Olayioye, M. A., Intracellular signaling pathways of ErbB2/HER-2 and family members, *J. Can. Res.* **2001**, *3*, 385, DOI: 10.1186/bcr327.
- [10] Nahta, R.; Yuan, L. X.; Zhang, B.; Kobayashi, R.; Esteva, F. J., Insulin-like growth factor-I receptor/human epidermal growth factor receptor 2 heterodimerization contributes to trastuzumab resistance of breast cancer cells, *J. Can. Res.* **2005**, *65*, 11118-11128, DOI: 10.1158/0008-5472.CAN-04-3841.
- [11] Spector, N.; Xia, W.; El-Hariry, I.; Yarden, Y.; Bacus, S., HER2 therapy. Small molecule HER-2 tyrosine kinase inhibitors, *Breast Cancer Res.*, **2007**, *9*, 205, DOI: 10.1186/bcr1652.
- [12] Telesco, S. E.; Radhakrishnan, R., Atomistic insights into regulatory mechanisms of the HER2 tyrosine kinase domain: a molecular dynamics study, *J. Bio. Phys.* **2009**, *96*, 2321-2334, DOI: <http://dx.doi.org/10.1016>.
- [13] Schulze, W. X.; Deng, L.; Mann, M., Phosphotyrosine interactome of the ErbB-receptor kinase family, *J. Mol. Syst. Biol.* **2005**, *1*, DOI: 10.1038/msb4100012.
- [14] Jones, R. B.; Gordus, A.; Krall, J. A.; MacBeath, G., A quantitative protein interaction network for the ErbB receptors using protein microarrays, *J. Nat.* **2006**, *439*, 168-174, DOI: 10.1038/nature04177.
- [15] Lin, S. -Y.; Makino, K.; Xia, W.; Matin, A.; Wen, Y.; Kwong, K. Y.; Bourguignon, L.; Hung, M. -C., Nuclear localization of EGF receptor and its potential new role as a transcription factor, *J. Nat. Cell. Biol.* **2001**, *3*, 802-808, DOI: 10.1038/ncb0901-802.
- [16] Wang, S. -C.; Lien, H. -C.; Xia, W.; Chen, I. -F.; Lo, H. -W.; Wang, Z.; Ali-Seyed, M.; Lee, D. -F.; Bartholomeusz, G.; Ou-Yang, F., Binding at and transactivation of the COX-2 promoter by nuclear tyrosine kinase receptor ErbB-2, *J. Cancer. Cell.* **2004**, *6*, 251-261, DOI: <http://dx.doi.org/10.1016>.
- [17] Williams, C. C.; Allison, J. G.; Vidal, G. A.; Burow, M. E.; Beckman, B. S.; Marrero, L.; Jones, F. E., The ERBB4/HER4 receptor tyrosine kinase regulates gene expression by functioning as a STAT5A nuclear chaperone, *J. Cell. Biol.* **2004**, *167*, 469-478, DOI: 10.1083/jcb.200403155.
- [18] Engel, R. H.; Kaklamani, V. G., HER2-positive breast cancer, *J. Drugs.* **2007**, *67*, 1329-1341, DOI: 10.2165/00003495-200767090-00006.
- [19] Sakai, K.; Mori, S.; Kawamoto, T.; Taniguchi, S.; Kobori, O.; Morioka, Y.; Kuroki, T.; Kano, K., Expression of epidermal growth factor receptors on normal human gastric epithelia and gastric carcinomas, *J. Natl Cancer Institute.* **1986**, *77*, 1047-1052, DOI: <https://doi.org/10.1093/jnci/77.5.1047>.
- [20] Uchino, S.; Tsuda, H.; Maruyama, K.; Kinoshita, T.; Sasako, M.; Saito, T.; Kobayashi, M.; Hirohashi, S., Overexpression of c-erbB-2 protein in gastric cancer, Its correlation with long-term survival of patients, *Cancer.* **1993**, *72*, 3179-3184, DOI: 10.1002/1097-142(19931201)72:11<3179:AID-CNCR2820721108>3.0.CO;2.
- [21] Yonemura, Y.; Ninomiya, I.; Yamaguchi, A.; Fushida, S.; Kimura, H.; Ohoyama, S.; Miyazaki, I.; Endou, Y.; Tanaka, M.; Sasaki, T., Evaluation of immunoreactivity for erbB-2 protein as a marker of poor short term prognosis in gastric cancer, *J. Can. Res.* **1991**, *51*, 1034-1038, DOI: Published February 1991.
- [22] Bookman, M. A.; Darcy, K. M.; Clarke-Pearson, D.; Boothby, R. A.; Horowitz, I. R., Evaluation of

- monoclonal humanized anti-HER2 antibody, trastuzumab, in patients with recurrent or refractory ovarian or primary peritoneal carcinoma with overexpression of HER2: a phase II trial of the Gynecologic Oncology Group, *J. Clin. Oncol.* **2003**, *21*, 283-290.
- [23] Pils, D.; Pinter, A.; Reibenwein, J.; Alfanz, A.; Horak, P.; Schmid, B.; Hefler, L.; Horvat, R.; Reinhaller, A.; Zeillinger, R., In ovarian cancer the prognostic influence of HER2/neu is not dependent on the CXCR4/SDF-1 signalling pathway, *J. Br. J. Cancer.* **2007**, *96*, 485-491, DOI: 10.1038/sj.bjc.6603581.
- [24] Steffensen, K. D.; Waldstrøm, M.; Jeppesen, U.; Jakobsen, E.; Brandslund, I.; Jakobsen, A., The prognostic importance of cyclooxygenase 2 and HER2 expression in epithelial ovarian cancer, *J. Int. J. Gynecol. Cancer.* **2007**, *17*, 798-807, DOI: 10.1111/j.1525-1438.2006.00855.x.
- [25] Scher, H. I., HER2 in prostate cancer-a viable target or innocent bystander? , *J. Ox. Univ. Press.* 2000, DOI: <https://doi.org/10.1093/jnci/92.23.1866>.
- [26] Signoretti, S.; Montironi, R.; Manola, J.; Altimari, A.; Tam, C.; Bubley, G.; Balk, S.; Thomas, G.; Kaplan, I.; Hlatky, L., Her-2-neu expression and progression toward androgen independence in human prostate cancer, *J. Natl Cancer Inst.* **2000**, *92*, 1918-1925, DOI: <https://doi.org/10.1093/jnci/92.23.1918>.
- [27] Medrano, J.; Barreiro, P.; Tuma, P.; Vispo, E.; Labarga, P.; Blanco, F.; Soriano, V., Risk for immune-mediated liver reactions by nevirapine revisited, *J. AIDS. Rev.* **2008**, *10*, 110-115.
- [28] Mirzaie, S.; Chupani, L.; Barzegari Asadabadi, E.; Shahverdi, A. R.; Jamalana, M., Novel inhibitor discovery against aromatase through virtual screening and molecular dynamic simulation: a computational approach in drug design, *Excell J.* **2013**, *12*, 168-183.
- [29] Mirzaie, S.; Monajjemi, M.; Hakhamaneshi, M. S.; Fathi, F.; Jamalana, M., Combined 3D-QSAR modeling and molecular docking study on multi-acting quinazoline derivatives as HER2 kinase inhibitors, *Excell J.* **2013**, *12*, 130.
- [30] Lagorce, D.; Sperandio, O.; Galons, H.; Miteva, M. A., FAF-Drugs2: free ADME/tox filtering tool to assist drug discovery and chemical biology projects, *BMC Bioinformatics.* **2008**, *9.1*, 396.
- [31] Mollica, A.; Mirzaie, S.; Costante, R.; Carradori, S.; Macedonio, G.; Stefanucci, A.; Dvoracsko, S.; Novellino, E., Exploring the biological consequences of conformational changes in aspartame models containing constrained analogues of phenylalanine, *J. Enzyme. Inhib. Med. Chem.* **2016**, *31*, 953-963, DOI: <http://dx.doi.org/10.3109/14756366.2015.1076811>.
- [32] Irwin, J. J.; Shoichet, B. K., ZINC- a free database of commercially available compounds for virtual screening, *J. Chem. Inf. Model.* **2005**, *45*, 177-182, DOI: 10.1021/ci049714.
- [33] Cortopassi, W. A.; Feital, R. J. C.; Medeiros, D. d. J.; Guizado, T. R. C.; França, T. C. C.; Pimentel, A. S., Docking and molecular dynamics studies of new potential inhibitors of the human epidermal receptor 2, *J. Mol. Simul.* **2012**, *38*, 1132-1142, DOI: <http://dx.doi.org/10.1080/08927022.2012.696113>.
- [34] Ishikawa, T.; Seto, M.; Banno, H.; Kawakita, Y.; Oorui, M.; Taniguchi, T.; Ohta, Y.; Tamura, T.; Nakayama, A.; Miki, H., Design and synthesis of novel human epidermal growth factor receptor 2 (HER2)/epidermal growth factor receptor (EGFR) dual inhibitors bearing a pyrrolo [3,2-d] pyrimidine scaffold, *J. Med. Chem.* **2011**, *54*, 8030-8050, DOI: 10.1021/jm2008634.
- [35] Schroeder, R. L.; Stevens, C. L.; Sridhar, J., Small molecule tyrosine kinase inhibitors of ErbB2/HER2/Neu in the treatment of aggressive breast cancer, *Molecules.* **2014**, *19*, 15196-15212, DOI: 10.3390/molecules190915196.
- [36] Gasteiger, J.; Marsili, M., Iterative partial equalization of orbital electronegativity-a rapid access to atomic charges, *J. Tetrahedron.* 1980, *36*, 3219-3228, DOI: [https://doi.org/10.1016/0040-4020\(80\)80168-2](https://doi.org/10.1016/0040-4020(80)80168-2).
- [37] Van Der Spoel, D.; Lindahl, E.; Hess, B.; Groenhof, G.; Mark, A. E.; Berendsen, H. J., GROMACS: fast, flexible, and free, *J. Comput. Chem.* **2005**, *26*, 1701-1718, DOI: 10.1002/jcc.20291.
- [38] Trott, O.; Olson, A. J., AutoDock Vina: improving the speed and accuracy of docking with a new scoring function, efficient optimization, and multithreading, *J. Comput. Chem.* **2010**, *31*, 455-461, DOI: 10.1002/jcc.21334.

- [39] Bas, D. C.; Rogers, D. M.; Jensen, J. H., Very fast prediction and rationalization of pKa values for protein-ligand complexes, *Proteins: Structure, Function, and Bioinformatics*. **2008**, *73*, 765-783, DOI: 10.1002/prot.22102. <https://doi.org/10.1016/j.jmfm.2005.12.005>.
- [40] Wang, J.; Wang, W.; Kollman, P. A.; Case, D. A., Automatic atom type and bond type perception in molecular mechanical calculations, *J. Mol. Graph. Model*. **2006**, *25*, 247-260, DOI:
- [41] Jorgensen, W. L.; Chandrasekhar, J.; Madura, J. D.; Impey, R. W.; Klein, M. L., Comparison of simple potential functions for simulating liquid water, *J. chem. phys.* **1983**, *79*, 926-935, DOI: <http://dx.doi.org/10.1063/1.445869>.
- [42] Darden, T.; York, D.; Pedersen, L., Particle mesh Ewald: An N-log(N) method for Ewald sums in large systems, *J. Chem. phys.* **1993**, *98*, 10089-10092, DOI: <http://dx.doi.org/10.1063/1.464397>.
- [43] Essmann, U.; Perera, L.; Berkowitz, M. L.; Darden, T.; Lee, H.; Pedersen, L. G., A smooth particle mesh Ewald method, *J. Chem. Phys.* **1995**, *103*, 8577-8593, DOI: <http://dx.doi.org/10.1063/1.470117>.
- [44] Bussi, G.; Donadio, D.; Parrinello, M., Canonical sampling through velocity rescaling, *J. Chem. Phys.* **2007**, *126*, 014101, DOI: <http://dx.doi.org/10.1063/1.2408420>.
- [45] Parrinello, M.; Rahman, A., Polymorphic transitions in single crystals: A new molecular dynamics method, *J. App. Phys.* **1981**, *52*, 7182-7190, DOI: <http://dx.doi.org/10.1063/1.328693>.
- [46] Humphrey, W.; Dalke, A.; Schulten, K., VMD: visual molecular dynamics, *J. Mol. Graph.* **1996**, *14*, 33-38, DOI: [https://doi.org/10.1016/0263-7855\(96\)00018-5](https://doi.org/10.1016/0263-7855(96)00018-5).
- [47] Kumari, R.; Kumar, R.; Lynn, A., g_mmpbsa A GROMACS Tool for High-Throughput MM-PBSA Calculations, *J. Chem. Inf. Model*. **2014**, *54*, 1951-1962, DOI: 10.1021/ci500020m.
- [48] Schmidt, M. W.; Baldridge, K. K.; Boatz, J. A.; Elbert, S. T.; Gordon, M. S.; Jensen, J. H.; Koseki, S.; Matsunaga, N.; Nguyen, K. A.; Su, S., General atomic and molecular electronic structure system, *J. Comput. Chem.* **1993**, *14*, 1347-1363, DOI: 10.1002/jcc.540141112.
- [49] Zhao, Y.; Schultz, N. E.; Truhlar, D. G., Design of density functionals by combining the method of constraint satisfaction with parametrization for thermochemistry, thermochemical kinetics, and noncovalent interactions, *J. Chem. Theory Comput.* **2006**, *2*, 364-382, DOI: 10.1021/ct0502763.
- [50] Zhao, Y.; Truhlar, D. G., The M06 suite of density functionals for main group thermochemistry, thermochemical kinetics, noncovalent interactions, excited states, and transition elements: two new functionals and systematic testing of four M06-class functionals and 12 other functionals, *Theoretical Chemistry Accounts: Theory, Computation, and Modeling (Theoretica Chimica Acta)*. **2008**, *120*, 215-241, DOI: 10.1007/s00214-007-0310-x.
- [51] Wang, W.; Hobza, P., Origin of the X-Hal (Hal = Cl, Br) Bond-Length Change in the Halogen-Bonded Complexes, *J. Phys. Chem. A*. **2008**, *112*, 4114-4119, DOI: 10.1021/jp710992h.
- [52] Müller-Dethlefs, K.; Hobza, P., Noncovalent interactions: a challenge for experiment and theory, *J. Chem. Rev.* **2000**, *100*, 143-168, DOI: 10.1021/cr9900331.
- [53] Keith, T. A., AIMAll.TK Gristmill Software, Overland Park KS, USA 2013.
- [54] Citri, A.; Gan, J.; Mosesson, Y.; Vereb, G.; Szollosi, J.; Yarden, Y., Hsp90 restrains ErbB-2/HER2 signalling by limiting heterodimer formation, *EMBO reports*. **2004**, *5*, 1165-1170, DOI: 10.1038/sj.embor.7400300.
- [55] Xu, W.; Yuan, X.; Xiang, Z.; Mimnaugh, E.; Marcu, M.; Neckers, L., Surface charge and hydrophobicity determine ErbB2 binding to the Hsp90 chaperone complex, *J. Nat. Struct. Mol. Biol.* **2005**, *12*, 120-126, DOI: 10.1038/nsmb885.
- [56] Kumar, K.; Anbarasu, A.; Ramaiah, S., Molecular docking and molecular dynamics studies on β -lactamases and penicillin binding proteins, *J. Mol. BioSyst.* **2014**, *10*, 891-900, DOI: 10.1039/C3MB70537D.
- [57] Aertgeerts, K.; Skene, R.; Yano, J.; Sang, B. C.; Zou, H.; Snell, G.; Jennings, A.; Iwamoto, K.; Habuka, N.; Hirokawa, A., Structural analysis of the mechanism of inhibition and allosteric activation of the kinase

- domain of HER2 protein, *J. Biol. Chem.* **2011**, *286*, 18756-18765, DOI: 10.1074/jbc.M110.206193.
- [58] Huse, M.; Kuriyan, J., The conformational plasticity of protein kinases, *J. Cell.* **2002**, *109*, 275-282, DOI: [https://doi.org/10.1016/S0092-8674\(02\)00741-9](https://doi.org/10.1016/S0092-8674(02)00741-9).
- [59] Trowe, T.; Boukouvala, S.; Calkins, K.; Cutler, R. E.; Fong, R.; Funke, R.; Gendreau, S. B.; Kim, Y. D.; Miller, N.; Woolfrey, J. R., EXEL-7647 inhibits mutant forms of ErbB2 associated with lapatinib resistance and neoplastic transformation, *Clin. Cancer Res.* **2008**, *14*, 2465-2475, DOI: 10.1158/1078-0432.CCR-07-4367.
- [60] Kutzelnigg, W., Atoms in Molecules. A Quantum Theory (Reihe: International Series of Monographs on Chemistry, Vol. 22.) Von RFW Bader. Clarendon Press, Oxford, 1990. XVIII, 438 S., geb.£ 50.00-ISBN 0-19-855168-1, *J. Angew. Chem.* **1992**, *104*, 1423-1423, DOI: 10.1002/ange.19921041040.
- [61] Espinosa, E.; Souhassou, M.; Lachekar, H.; Lecomte, C., Topological analysis of the electron density in hydrogen bonds, *J. Acta Cryst. B.* **1999**, *55*, 563-572, DOI: <https://doi.org/10.1107/S0108768199002128>.
- [62] Gatti, C.; Saunders, V.; Roetti, C., Crystal field effects on the topological properties of the electron density in molecular crystals: The case of urea, *J. Chem. Phys.* **1994**, *101*, 10686-10696, DOI: <http://dx.doi.org/10.1063/1.467882>.
- [63] Cremer, D.; Kraka, E., Chemical Bonds without Bonding Electron Density-Does the Difference Electron-Density Analysis Suffice for a Description of the Chemical Bond?, *J. Angew. Chem. Int. Ed.* **1984**, *23*, 627-628, DOI: 10.1002/anie.198406271.
- [64] Jenkins, S.; Morrison, I., The chemical character of the intermolecular bonds of seven phases of ice as revealed by ab initio calculation of electron densities, *J. Chem. Phys. Lett.* **2000**, *317*, 97-102, DOI: [https://doi.org/10.1016/S0009-2614\(99\)01306-8](https://doi.org/10.1016/S0009-2614(99)01306-8).
- [65] Grabowski, S. J., High-level *ab initio* calculations of dihydrogen-bonded complexes, *J. Phys. Chem. A.* **2000**, *104*, 5551-5557, DOI: 10.1021/jp993984r.
- [66] Eshtiagh-Hosseini, H.; Beyramabadi, S. A.; Morsali, A.; Mirzaei, M.; Chegini, H.; Elahi, M.; Naseri, M. A., Synthesis, characterization and intramolecular proton transfer of 3,3'-dihydroxy-4,4'-[5-methyl-1, 3-phenylenebis (nitrilomethylidyne)]-bis-phenol, *J. mol. struct.* **2014**, *1072*, 187-194, DOI: <https://doi.org/10.1016/j.molstruc.2014.05.003>.
- [67] Cortés-Guzmán, F.; Bader, R. F., Complementarity of QTAIM and MO theory in the study of bonding in donor-acceptor complexes, *J. Coord. Chem. Rev.* **2005**, *249*, 633-662, DOI: <https://doi.org/10.1016/j.ccr.2004.08.022>.
- [68] Astani, E. K.; Heshmati, E.; Chen, C. -J.; Hadipour, N. L., A theoretical study on the characteristics of the intermolecular interactions in the active site of human androsterone sulphotransferase: DFT calculations of NQR and NMR parameters and QTAIM analysis, *J. Mol. Graph. Model.* **2016**, *68*, 14-22, DOI: <https://doi.org/10.1016/j.jmgm.2016.06.002>, DOI: <https://doi.org/10.1016/j.jmgm.2016.06.002>.
- [69] Vener, M.; Manaev, A.; Egorova, A.; Tsirelson, V., QTAIM Study of Strong H-Bonds with the O-H-A Fragment (A = O, N) in Three-Dimensional Periodical Crystals, *J. Phys. Chem. A.* **2007**, *111*, 1155-1162, DOI: 10.1021/jp067057d.
- [70] Chegini, H.; Beyramabadi, S. A.; Morsali, A.; Saberi, M.; Lotfi, M., QTAIM study of substituent effects on the intramolecular hydrogen bond in 3, 3'-dihydroxy-4,4'-[5-methyl-1,3-phenylenebis(nitrilomethylidyne)]-bis-phenol, *J. Mol. Struct.* **2015**, *1083*, 1-9, DOI: <https://doi.org/10.1016/j.molstruc.2014.11.031>.
- [71] Lu, J.; Zhang, Z.; Ni, Z.; Shen, H.; Tu, Z.; Liu, H.; Lu, R., QM/MM-PB/SA scoring of the interaction strength between Akt kinase and apigenin analogues, *J. Comput. Biol. Chem.* **2014**, *52*, 25-33, DOI: <https://doi.org/10.1016/j.compbiolchem.2014.07.002>.
- [72] MM, S. M., Molecular dynamics and high throughput binding free energy calculation of anti-actin anticancer drugs-new insights for better design, *J. Comput. Biol. Chem.* **2016**, *64*, 47-55.